ELECTRON TECHNOLOGY
ISSN 1897-2381
http://www.ite.waw.pl/etij/
Internet Journal

TRANSMISSION ELECTRON MICROSCOPY OF In(Ga)As QUANTUM DOT STRUCTURES

J. KĄTCKI[1], J. RATAJCZAK[1], A. ŁASZCZ[1], F. PHILLIPP[2], C. PARANTHOEN[3], X. L. CHENG[3 a], A. FIORE[3 b], A. PASSASEO[4], R. CINGOLANI[4]

[1]Institute of Electron Technology, al. Lotników 32/46, 02-668 Warszawa, Poland
[2]Max-Planck-Institut für Metallforschung, Heisenbergstr. 3, D-70569 Stuttgart, Germany
[3]Institut de Photonique et d'Electronique Quantique Ecole Polytechnique Fédérale de Lausanne, CH 1015 Lausanne, Switzerland
[4]National Nanotechnology Laboratory - INFM, c/o Dipartimento di Ingegneria dell'Innovazione, Università di Lecce, via Arnesano, 73100 Lecce, Italy

Received July 31, 2003; Published September 1, 2003

ABSTRACT

The application of transmission electron microscopy (TEM) to the investigation of In(Ga)As quantum dot (QD) structures grown on GaAs substrates is reviewed. Using various examples of the QD structures the advantages of using TEM for the analysis of QDs are presented. From plan-view TEM images the areal density of dots can be determined in real structures where QDs are embedded in the structure. Cross-sectional TEM images inform us about the real geometry of the structure, the shape, width and height as well as the distribution of QDs. It is especially useful for the investigations of multilayer QD structures.

1. Introduction

The demonstration that self-assembled In(Ga)As quantum dots (QDs) grown on gallium arsenide can emit at 1.3 μm [1] opened very promising opportunities. Such heterostructures can be grown on a GaAs substrate using conventional, single-run epitaxial growth technique, fully compatible with industrial production. This is why significant efforts have been recently made to develop the growth of In(Ga)As QDs structures using both molecular beam epitaxy (MBE) [2−7] and metal-organic chemical-vapour deposition (MOCVD) [8−13].

In In(Ga)As QD structures one or few layers of In(Ga)As QDs are located in a GaAs resonant cavity. During optimization of the growth process of QD structures it is very important to know the shape, the size and the density of dots as well as their distribution, since these parameters influence the device performance. A very useful tool for analysing such embedded objects like QDs is a transmission electron microscope (TEM).

[a]Present address: Bell Laboratories, Lucent Technologies Inc., 600 Mountain Ave., Murray Hill, NJ, 07974, USA.
[b]Permanent address: Institute of Photonics and Nanotechnology, CNR, via del Cineto Romano 42, 00156 Roma, Italy.

In this paper, the application of TEM to the investigation of In(Ga)As QD structures grown on GaAs substrates is reviewed. Employing various examples of QD structures grown both by MBE and MOCVD, benefits of using TEM for the QD analysis are demonstrated.

2. Experimental

QD samples were grown in two ways: i) by solid source molecular beam epitaxy (SS-MBE) and ii) by low-pressure MOCVD in both cases on (100)-oriented GaAs substrates.

The procedure of growing MBE InAs QD samples was as follows. After oxide removal, a 0.5 μm thick GaAs buffer layer was grown. QDs were then formed, by the deposition of 2.9 monolayers (ML) of InAs, as observed by the abrupt change from a streaky to a spotty RHEED diffraction pattern. These QDs may be covered by a 5 nm $In_{0.15}Ga_{0.85}As$ capping layer in order to shift the wavelength to 1.3 μm. Several samples have been grown, from single QD layer (with and without InGaAs capping layer), to several QD layers (up to seven) separated by 40 nm of GaAs. Each QD sample was enclosed in the same structure, i.e. inserted at the centre of

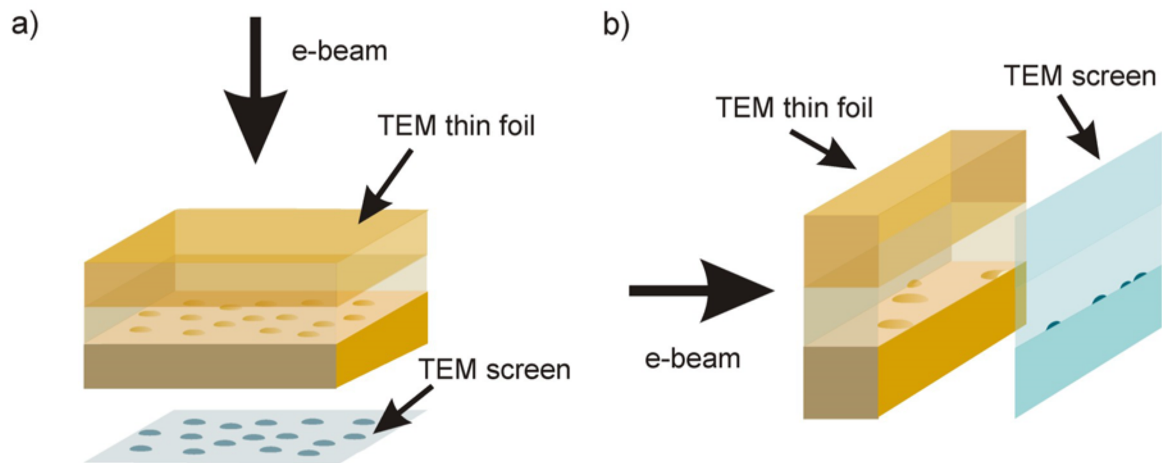

Fig. 1. Imaging of QDs in a TEM: a) plan-view sample; b) cross-sectional sample.

a 200 nm thick GaAs layer, surrounded by 20 nm thick AlAs layers.

Low-pressure MOCVD $In_xGa_{1-x}As$ QD samples were grown at T = 550°C. The sample structures consist of a single InGaAs dot layer inserted into an $In_xGa_{1-x}As$ barrier, grown over an $Al_{0.4}Ga_{0.6}As$ cladding layer (1.2 µm thick). In the samples studied in the present work the InAs mole fraction in the barrier is varied between x = 0.5 and x = 0.1. The island are formed after the deposition of 4 MLs of $In_xGa_{1-x}As$, at a growth rate of 1 MLs/sec and AsH_3 partial pressure of $1.4\cdot10^{-1}$ mbar. In the uncovered samples, the growth is stopped after the deposition of the QD layer and immediately cooled down under AsH_3 stabilization. For the capped samples, the growth is stopped for 90 second before the deposition of the InGaAs barrier. More details about the growth of the QD layers are described elsewhere [10, 11]. The described growth conditions lead to structures with a QD density of around $3\cdot10^{10}$ cm^{-2} and narrow size distribution.

Cross-sectional TEM samples were prepared by the method described by KĄTCKI ET AL. [14]. The specimens were studied in the following transmission electron microscopes: JEM-200CX operating at 200 keV (Institute of Electron Technology) and JEM-4000FX operating at 400 keV (Max-Planck-Institut fűr Metallforschung).

3. Results and discussion

Currently, QDs can be grown in a controllable way. Under the Stransky-Krastanov growth mode the formation of QDs is driven by the strain during epitaxial growth of In(Ga)As on the GaAs substrate as the deposited layer exceeds a critical thickness. Then, the growth mode changes from a two-dimensional growth to a three-dimensional growth and the strain is relieved elastically without formation of lattice defects.

After the formation, QDs can be easily characterized by topographical techniques (for example: Atomic Force Microscopy – AFM). However, in a real structure subsequent layers are deposited on the QD layer and QDs are embedded in a matrix, Topographic techniques are, here, useless. In QD structures studied in our project quantum dots are typically located 100 – 200 nm below the structure surface. The electron beam in a transmission electron microscope operating at 200 kV can go through a thin-foil sample not thicker than 400 nm. **A TEM plan-view sample** from a QD structure can be prepared by thinning the sample from the back side. A schematic drawing of such a sample is shown in Fig. 1a. The orientation of the sample surface is of {100} type. Since during the TEM observation of the plan-view sample the electron beam traverses the specimen almost perpendicularly to the surface, the image visible on a TEM screen is the <100> type projection of the sample (Fig. 1a). From such an image we can learn about the areal density and distribution of QDs.

Plan-view images inform us about the density and distribution of QDs but the information about the QD height, width (diameter) and the shape is missing, We can see a symmetrical dark contrast but the measurement of the QD width from this contrast is not sure. For this purpose, much better are TEM observations of **cross-sectional samples** prepared from QD structures. A schematic drawing of such a sample is shown in Fig. 1b. In this case, on a TEM screen an image being a cross-section of the structure is observed. From that kind of image one can measure geometrical parameters of the structures such as thicknesses of layers, sizes and the linear distribution of phase objects located in a TEM section.

In Fig. 2a a schematic drawing of a MBE grown QD sample is presented. A cross-sectional TEM image of this sample is shown in Fig. 2b. On this image GaAs and AlAs layers can be easily

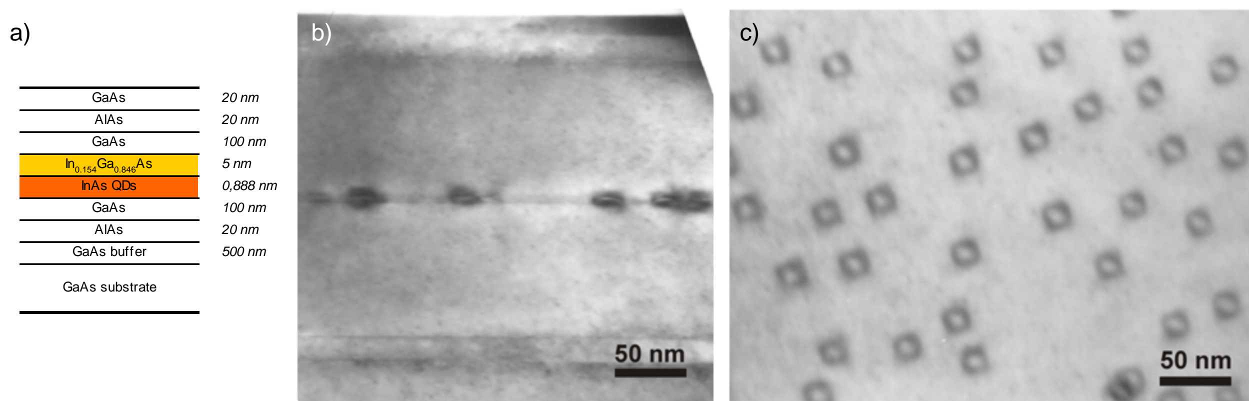

Fig. 2. Analysis of QDs in a TEM: a) schematic drawing; b) cross-sectional image; c) plan-view image.

distinguished since the contrast from AlAs layers is brighter than from layers of GaAs. The exact thicknesses of AlAs and GaAs layers measure from the TEM image are 19 nm and 100 nm respectively. A layer of InAs QDs is located between two GaAs layers. It is covered by a 5 nm thick $In_{0.154}Ga_{0.846}As$ capping layer. In case of this sample QDs were grown directly on GaAs. Bright contrast from QDs is surrounded by dark contrast from strain formed in matrix around the dots (especially above and below the dots). The width of the QDs taken from the image is about 20 nm.

Figure 2c shows a TEM plan-view image of the QD sample. In the sample being studied the QDs are located approximately 140 nm below the structure surface. Such a specimen requires thinning only from the back-side. The strain contrast around the dots is easily distinguishable. Such contrast can be obtained by setting two diffracted beams in exact Bragg conditions. It is visible as dark symmetrical shapes. The areal density of QDs can be determined by counting the number of QDs in a certain square area. The smaller magnifications are better for this purpose since the area from which we count is bigger and the accuracy of this measurement is better. For this sample the areal density of QD is 302 dots/μm^2. From the TEM cross-section the linear density of QDs can be measure. In case of significant amount of dots this density is proportional to the areal density of dots. Similarly as in case of the areal density, the smaller magnification the better accuracy of measurement.

We can assume that the thickness of a thin foil constituting a cross-section of the QD structure is below 50 nm. In order to better understand what we see in the cross-sectional image, on the plan-view image shown in Fig. 2c we can imagine two parallel lines, one 50 nm away from another drawn in Fig.2b. Since, as we found, the distribution of QDs is uniform and the QD density is high enough, without being mistaken we can say that a cross-sectional sample should contain in its bulk many full-sized QDs.

In Fig. 3a a schematic drawing of another MBE grown QD sample is shown. The difference between this one and previously discussed (Fig. 2a) is that the QDs, here, were grown on a 5 nm thick $In_{0.154}GaAs_{0.846}As$ layer, while in case of the sample discussed above (Fig. 2) the QDs were grown directly on GaAs. Similarly as in a sample previously discussed the QDs were covered by a 5 nm thick $In_{0.154}Ga_{0.846}As$ capping layer.

Figures 3b and 3c show bright-field (BF) and dark-field (DF) cross-sectional TEM images of this sample, respectively. In the BF image shown in Fig. 3b a contrast on QDs is dominated by strain contrast, which can be significantly decreased using DF images (Fig. 3c). In a DF image the QDs are white, while InGaAs “matrix” is black. From such an

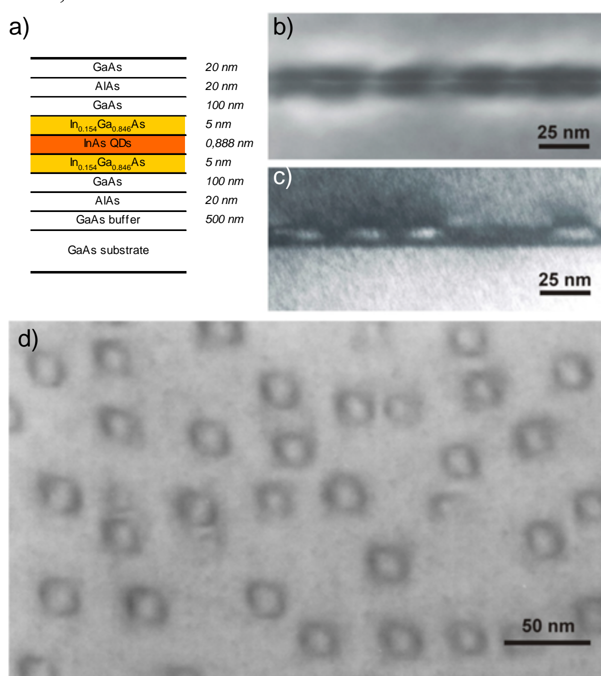

Fig. 3. MBE grown QD samples: a) BF image; b) DF image; c) plan-view image.

image a shape of dots can be determined. In this case it is typical for the MBE growth, a half-lens shape. Assuming that the QD located rightmost on the image (Fig. 3c) was totally included in a thin foil (so we see its full projection), we can measure its width. It is approximately 25 nm.

In Fig. 3d a plan-view image of this sample is presented. Similar contrast as in Fig. 2c is observed. Please note that the magnification of this image is higher than ones shown in Fig. 3b and c but the same as in Fig. 2c. The areal density of QD is here 450 dots/μm^2.

In order to compare the areal density of dots in two samples grown by MBE directly on a GaAs layer with (Fig. 4a) and without (Fig. 4c) a 5 nm thick $In_{0.15}GaAs_{0.85}As$ capping layer plan-view samples were prepared. Plan-view TEM images of dots with and without an $In_{0.15}GaAs_{0.85}As$ capping layer are shown in Figs. 4b and d, respectively. The areal density of QDs in case of using an $In_{0.15}GaAs_{0.85}As$ layer as a cap is 276 dots/μm^2, while in case of uncapped dots it is 364 dots/μm^2. We deduce that capping slightly reduces the dot density, possibly due to In diffusion along the growth plane during capping. We expect this mechanism to strongly depend on actual growth conditions.

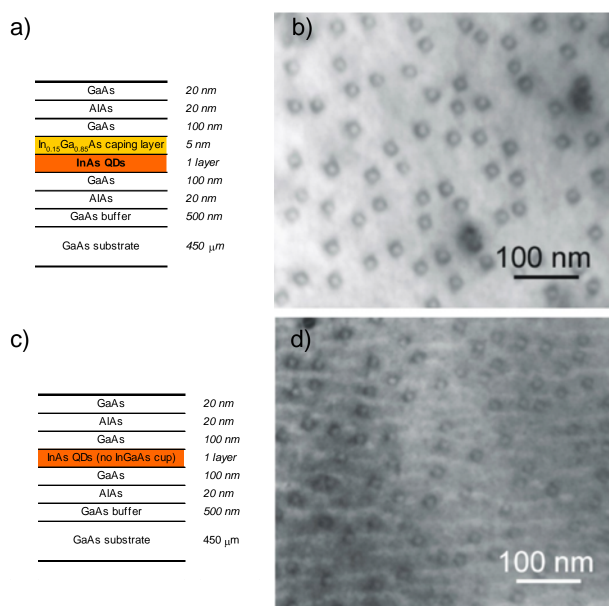

Fig. 4. Comparison of the areal density of QDs in MBE grown samples: a) InGaAs capped; b) no InGaAs cap.

In case of QD structure with few layers of QDs, plan-view TEM images do not provide satisfactory information. Then, all necessary information like the density and distribution of QDs should be taken from cross-sectional TEM images. Cross-sectional TEM images deliver also additional information on alignment of dots and their presence on a certain level.

In Fig. 5a a schematic drawing of a structure with three layers of QDs is shown. QD layers were separated, here, by a 10 nm-thick GaAs spacer layer. Each QD layer was grown on a GaAs layer and capped by a 5 nm thick $In_{0.15}GaAs_{0.85}As$ layer. Two samples with this geometry were grown. The difference between these samples consists in the modification of the growth stoichiometry in upper QD layers. In the samples with "modified" stoichiometry, the amount of InAs in the second and the third layer was decreased (in comparison to the first layer) while in the samples with "conventional" stoichiometry amount of InAs in all three layers was the same. In Fig. 5b and c cross-sectional TEM images of these samples are shown. In both samples QDs are vertically aligned. This is due to the residual

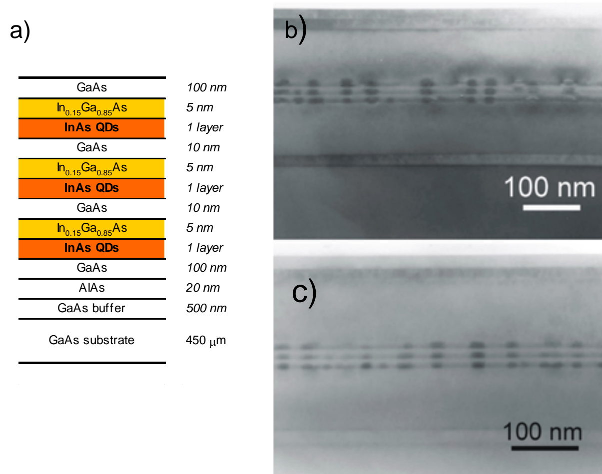

Fig. 5. Comparison of the MBE growth of QDs: a) schematic drawing; b) conventional stoichiometry; c) modified stoichiometry.

strain in the spacer layer, which favours nucleation on top of existing dots. In the sample shown in Fig. 5c QD columns are distributed more regularly. In both samples we observed areas where QDs were formed only in the first layer, but in the second and the third layer they are absent. In the sample grown in "conventional" way one can observe that the upper layer dots are bigger than of those located in the first layer. The higher the dot is located the bigger it is. Modification of growth parameters decreased the differences between the dot size (Fig. 5c).

The sizes of QDs in subsequent layers of a specimen with "modified" stoichiometry are almost equal. In certain cases upper dots are absent. In Fig. 6 a lattice image of a column (stack) of dots is shown. The lattice images were done in the [110] direction. No lattice defects are observed around dots.

In Fig. 7a a TEM cross-section of an MBE grown structure containing 7 layers of QDs with 40 nm-thick GaAs spacers is presented. The QDs in this sample were grown directly on GaAs. Each layer of QDs was capped by a 5 nm thick $In_{0.15}GaAs_{0.85}As$ layer. In Fig. 7b a schematic drawing of a sample is shown. The densities of dots in all layers excluding the top one are equal and no alignment of dots is observed, due to the thicker spacer layer. The QD density in the top layer is lower than in other ones.

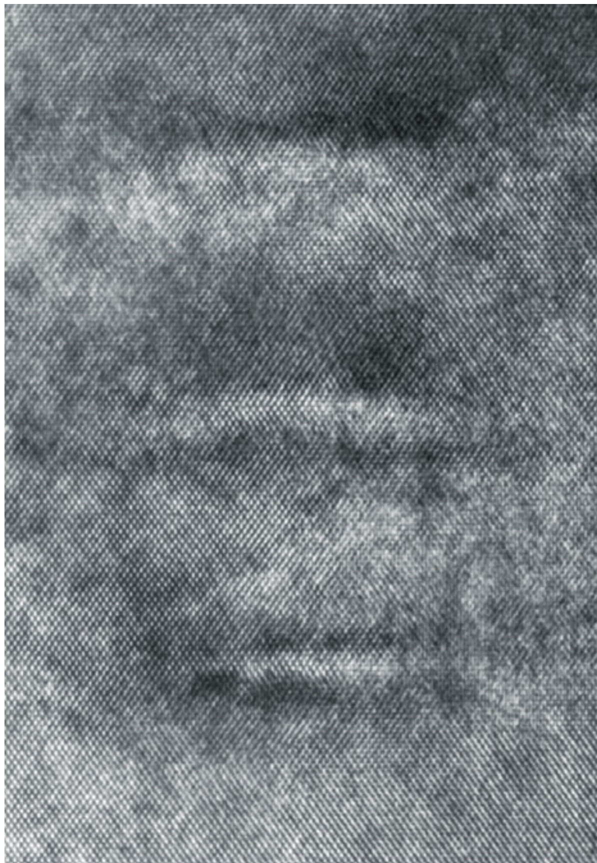

Fig. 6. Lattice image of 3-layer QD stack grown by MBE.

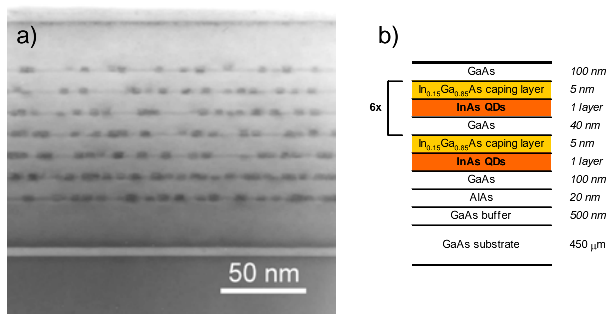

Fig. 7. Seven-layers QD specimen grown by MBE.

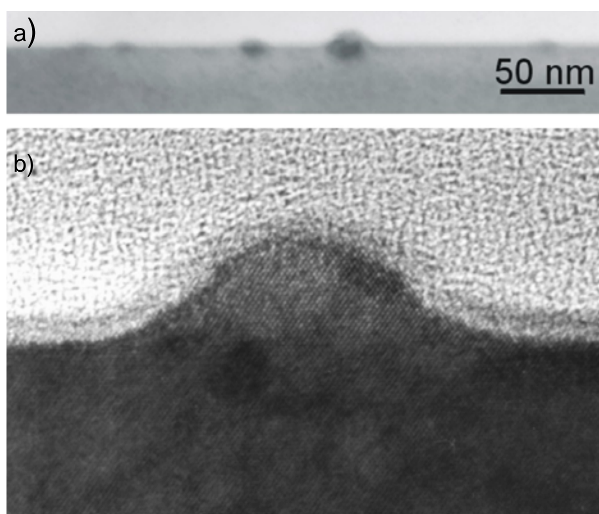

Fig. 8. As-grown MOCVD grown QDs: a) general cross-sectional view; b) <110> type lattice image of a single dot.

The observation of TEM cross-sections of QD structures allows to determine a shape of the QDs. One method is the observation of DF images (Fig. 3c). Another method is the observation of lattice images of the dots. In Fig. 8a a cross-sectional TEM image of an as-grown QDs is visible. QDs in this sample were grown by MOCVD of 4ML of InGaAs on a 4nm thick In0.1Ga0.9As. Figure 8b shows a <110>-type lattice image of a single QD.

After growing subsequent layers on QDs, the shape of QDs changes. The QDs become more flat. In Fig. 9a a <110>-type lattice image of a MOCVD grown QD is shown. QDs in this sample were grown by deposition of 4ML InGaAs layer on a 3 nm thick $In_{0.05}Ga_{0.95}As$ layer and capped by a 5 nm thick $In_{0.05}Ga_{0.95}As$ capping layer. In Fig. 9a a typical, for the MOCVD growth, shape of a truncated pyramid is observed. Symmetrical growth facets can be distinguished. Similar shapes of MOCVD dots were found in [11] and [12] by observation of <100> type lattice images. Growth facets visible in Fig. 9a (<110> type projection) are not so steep as in case of <100> type projection, shown in ref. [12]. They are located in {551} type crystallographic planes which are inclined at an angle of 24° to the (001) plane (the dot basis).

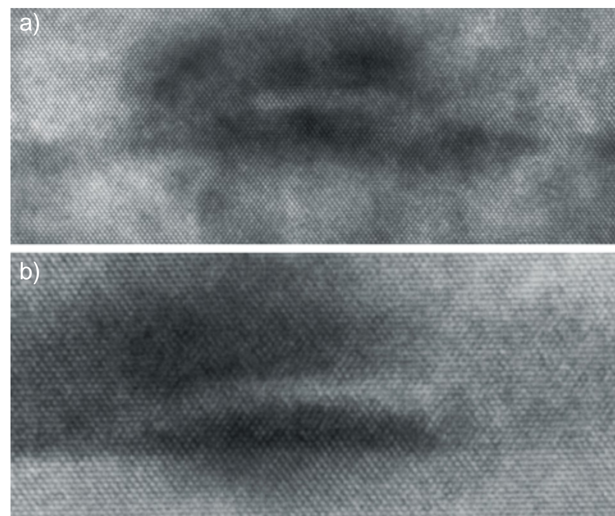

Fig. 9. <110> type lattice images grown by: a) MOCVD and b) MBE.

The shape of MBE grown QDs differs from the shape of those grown by MOCVD. For MBE grown QD samples, the typical shape of the QD is a half-lens. In Fig. 9b a <110>-type lattice image of a MBE grown QD is shown. The description of this sample is given in Fig. 5a. The QD shown in Fig. 9b was grown directly on GaAs and was capped by a 5 nm thick $In_{0.15}GaAs_{0.85}As$ layer.

3. Conclusions

In this paper the advantages of the application of transmission electron microscopy for optimization of QD growth is discussed. From plan-view TEM

images the areal density of dots can be determined. This technique allows to observe QDs both on the sample surface and embedded in the structure. Cross-sectional TEM images inform us about the real geometry of the structure, the shape, width and height as well as the distribution of QDs. It is especially useful for the investigations of multilayer QD structures.

Acknowledgment

This publication is based on the work sponsored by the European Commission under the project "*Gallium Arsenide Second Window Quantum-Dot Lasers*" (IST-1999-10450 GSQ) as well as by the Swiss National Science Foundation and the Polish Government. HRTEM studies were carried out due to the co-operation project between the IET and the MPI-MF according to executive protocols to inter-government agreements signed with the governments of Poland and Germany. The authors are very much indebted to Ms D Szczepańska and Mr J Gazda for assistance in specimen preparation and Ms J Wiącek for careful preparation of micrographs.

REFERENCES

1. D. L. HUFFAKER, G. PARK, Z. ZOU, O.B. SHCHEKIN, D. G. DEPPE, *1.3 μm Room-Temperature GaAs-Based Quantum-Dot Laser*, Appl. Phys. Lett., 1998, **73**, 2564.
2. D. BIMBERG, M. GRUNDMANN, N. N. LEDENTSOW, S. S. RUVIMOV, P, WERNER, U. RICHTER, J. HEYDENREICH, V. M. USTINOV, P. S. KOP'EV, Zh. I. ALFEROV, *Self-Organization Processes in MBE-Grown Quantum Dot Structures*, Thin Solid Films, 1995, **267**, 32–36.
3. D. LEONARD, S. FAFARD, K. POND, Y.H. ZHANG, J.L. MERZ, P.M. Petroff, Structural and Optical Properties of Self-Assembled InGaAs Quantum Dots, J. Vac. Sci & Technol. 1994, 12, 2516–2520.
4. H. ISHIKAWA, H. SHOJI, Y. NAKATA, K. MUKAI, M. SUGAWARA, M. EGAWA, N. OTSUKA, Y. SUGIJAMA, M. FUTATSUGI, N. YOKOYAMA, *Self-Organized Quantum Dots and Quantum Dot LASERs* (invited), J. Vacuum Sci. Technol. A, 1998, 16, 794.
5. V. M. USTINOV, A. Yu. EGOROV, A. R. KOVSH, A. E. ZHUKOV, M.V. MAXIMOV, A.F. TSATSUL'NIKOV, N. Yu. GORDEEV, S.V. ZAITSEV, Yu.M. SHERNYAKOV, N. A. BERT, P. S. KOP'EV, Zh. I. ALFEROV, N. N. LEDETSOV, J. BOHRER, D. BIMBERG, A. O. KOSOGOV, P. WERNER, U. GOSELE, *Low-Threshold Injection Lasers Based On Vertically Coupled Quantum Dots*, J. Cryst. Growth, 1997, 175/176, 689–695.
6. K. MUKAI, Y. NAKATA, K. OTSUBO, M. SUGAWARA, N. YOKOYAMA, H. ISHIKAWA, *High Characteristic Temperature of Near 1.3-mm InGaAs/GaAs Quantum-Dot Lasers at Room Temperature,* Appl. Phys. Lett., 2000, **76**, 3349.
7. J. X. CHEN, A. MARCUS, A. FIORE, U. OESTERLE, R. P. STANLEY, J. F. CARLIN, R. HOUDRE, L. LAZZARINI, L. NASI, M. T . TODARO, E. PISCOPIELLO, R. CINGOLANI, M. CATALANO, J. KATCKI, J. RATAJCZAK*, Tuning InAs/GaAs Quantum Dot Properties under Stranski-Krastanov Growth Mode for 1.3 Micrometers Applications*, J. Appl. Phys., 2002, **91**, 6710–6716.
8. J. OSHINOWO, M. NISHIOKA, S. ISHIDA, Y. ARAKAWA, *Highly Uniform InGaAs/GaAs Quantum Dots (~15 nm) by Metalorganic Chemical Vapor Deposition*, Appl.Phys. Lett. 1994, 65, 1421-1423.
9. J. BLOCH, J. SHAH, W. S. HOBSON, J. LOPATA, S. N. G. CHU, *Room-Temperature 1.3 μm Emission from InAs Quantum Dots Grown by Metal Organic Chemical Vapor Deposition*, Appl. Phys. Lett, 1999, **75**, 2199–2201.
10. A. PASSASEO, G. MARUCCIO, M. DE VITTORIO, R. RINALDI, R. CINGOLANI, M. LOMASCOLO, *Wavelength Control from 1.25 to 1.4 μm in $In_xGa_{1-x}As$ Quantum Dot Structures Grown by Metal Organic Chemical Vapor Deposition*, Appl. Phys. Lett. 2001, **78**, 1382–1384.
11. A. PASSASEO, R. RINALDI, M. LONGO, S. ANTONACI, A. L. CONVERTINO, R. CINGOLANI, A. TAURINO, M. CATALANO, *Structural Study of InGaAs/GaAs Quantum Dots Grown by Metalorganic Chemical Vapor Deposition for Optoelectronic Applications at 1.3 Micrometers*, J. Appl. Phys., 2001, **89**, 4341–4348.
12. M. DE GIORGI, A. PASSASEO, R. RINALDI, T. JOHAL, R. CINGOLANI, A. TAURINO, M. CATALANO, P. CROZIER, *Nanoscale Compositional Fluctuations in Single InGaAs/ /GaAs Quantum Dots*, phys. stat. sol. (b) , 2001, 224, 17–20.
13. A. PASSASEO, G. MARUCCIO, M. DE VITTORIO, S. DE RINALDIS, T. TODARO, R. RINALDI, R. CINGOLANI, *Dependence of the Emission Wavelength on the Internal Electronic Field in Quantum-Dot Laser Structures Grown by Metal-Organic Chemical-Vapor Deposition*, Appl. Phys. Lett, 2002, 79, 1435–1437.
14. J. KĄTCKI, J. RATAJCZAK, M. MALĄG, M. PISKORSKI, [in]: *Microscopy of Semiconducting Materials 1995 (A.G. Cullis*, A. Staton-Bevan, Eds.), Inst. Phys. Ser. 146, Inst. Phys., Bristol, 1995, 273–276.